FEASIBILITY STUDY ON REDUCING PIXEL RESOLUTION OF RAW HDR IMAGES FOR CALIBRATION OF SKY LUMINANCE MEASUREMENT

BY

Rex Jeffries

Submitted to the graduate degree program in Architectural Engineering and the Graduate Faculty of the University of Kansas in partial fulfillment of the requirements for the degree of Master of Science.

_____
Chairperson Dr. Hongyi Cai

_____
Dr. Mario Medina

_____
Dr. Jae D. Chang

Date Defended: 05/09/2016

The Thesis Committee for Rex Jeffries

certifies that this is the approved version of the following thesis:

FEASIBILITY STUDY ON REDUCING PIXEL RESOLUTION OF RAW HDR IMAGES FOR CALIBRATION OF SKY LUMINANCE MEASUREMENT

_____

Chairperson Dr. Hongyi Cai

Date approved: 06/13/2016

ABSTRACT

In the past, measuring the luminance distribution of the sky and the sun was done with either a sky scanner or a luminance meter. The conventional measurement methods are time consuming at low measurement resolution (with a maximum of 145 data points on the entire upper hemisphere), thus, cannot capture real-time changes typically seen with natural daylight. To solve this problem, a camera-array-based measurement technology was recently introduced by the University of Kansas lighting research laboratory to capture the spatial and temporal luminance distributions of the celestial hemisphere. This technique uses high dynamic range (HDR) photogrammetry for luminance mapping of the sky and the sun simultaneously. With two cameras mounted next to one another on a Sky Measurement Tripod Head developed in the lighting research laboratory, the sky and the sun are measured, respectively, by each camera.

However, one issue that still remains with this type of data collection is the storage and treatment of big data embedded in the HDR images generated in the field. Each HDR image has a file size of approximately 40-50 MB, while the retrieved 18 million luminance data in text file format could have a file size of approximately 400-500 MB. Given at least hourly measurements for real-time sky conditions from sunrise to sunset, it is very tedious to deal with such large amounts of data that challenge the speed and storage capacity of current computation facilities. To solve this problem, the present research study was aimed to explore the feasibility of reducing pixel resolutions in the laboratory of raw HDR images taken in the field, in the hopes of speeding up the data treatment process of the sky and the sun luminance measurement while still maintaining an adequate degree of accuracy.

An experiment was carried out at the Clinton State Park in Lawrence, KS at 1:30 pm on October 4th, 2015 to evaluate the null hypothesis that reducing the pixel resolution of the HDR images in the laboratory would not compromise the overall value of the obtained data. Two Canon digital cameras EOS Rebel T2i fitted with Sigma 4.5mm F2.8 EX DC HSM Circular Fisheye lenses were mounted side by side on a custom designed Sky Measurement Tripod Head to take measurements of the celestial sky using the HDR photography. One camera was mounted without a neutral density filter and was used to capture the luminance distribution of the sky while the other camera was equipped with a neutral density filter of 1/1000 and used to capture the luminance of the sun and its corona. The luminance data embedded in each of the two HDR images were later extracted in Radiance and outputted to Microsoft Access and Excel for the follow-up data treatment. It was discovered that the amount of data obtained from the cameras was very large and nearly impossible to handle in Microsoft Access or Excel due to their limited computation capacity of 18 million rows of data. This study then reduced such big data during the data extraction process in the laboratory by lowering the pixel resolutions of the raw HDR images obtained in the field. The size of the HDR images was reduced from 18 million data points to merely 270,500 data points. The reduced datasets were then treated using Excel spreadsheets containing pre-developed equations. Calibration Factor (CF) values were calculated by comparing the actual horizontal illuminance measured using an illuminance meter to the calculated illuminance from the sky and sun luminance data embedded in the synthesized HDR image.

In theory, the CF ratio should be close to 1.0 indicating the robust data collection and treatment process was carried out with minimal error. In the present study, the CF

value obtained during the laboratory data treatment was close to 0.05, indicating the dataset was improperly manipulated during the reduction process of pixel resolutions. Photometric calibrations using such a CF value (0.05) would lead to extraction of only 5% of the true luminance distributions of the sky and the sun. As a result, it is deemed inappropriate to reduce the pixel resolution of raw HDR images in the laboratory after the field measurement, since such a reduction found in this study is associated with a loss of useful data for luminance mapping of the sky and the sun.

Further research to be conducted in the Lighting Research Lab will evaluate two possible ways to solve this problem. The first solution is to capture the HDR images with lower pixel resolutions by directly adjusting the camera settings in the field, which is not the optimal solution but recommended given the otherwise resulting big data and the limitations of current computing facilities. The second method is to conduct the data treatment in a more powerful computing software such as Matlab without reduction of the original 18 million pixels embedded in the HDR images.

Keywords: High dynamic range, HDR, Camera-array-based measurement, Calibration Photogrammetry, Pixel Reduction, Calibration Factor Values, Matlab

ACKNOWLEDGEMENTS

I would like to first thank the chairperson of my committee, Dr. Hongyi Cai, for advising me this past year during my completion of the graduate degree program. His critical thinking and passion for the lighting industry inspired me throughout my education at the University of Kansas. I enjoyed taking on this challenging research topic in order to help advance his studies in HDR photography.

In addition, I would like to thank my committee members, Dr. Mario Medina and Dr. Jae Chang. These professors were involved throughout my education in the undergraduate program at the University of Kansas, and they continued to have an impact as I continued my education. Dr. Chang helped expand my attention to detail and design in architectural studio while Dr. Medina taught me the importance of efficient energy management in the built environment. Without such great guidance from the hard-working and talented faculty at the University of Kansas, this study would not be possible.

Thanks to the University of Kansas, the Architectural Engineering program, and the CEAE department for giving me the opportunity to have an impact in this research area. I have enjoyed every step of the way, and I am eager to test my skills in the professional setting outside of academia.

NOMENCLATURE

κ	*Camera yaw angle around Z axis*
η	*Camera pitch angle around X axis*
φ	*Camera roll angle around Y axis*
$(\kappa_0, \eta_0, \varphi_0)$	*Camera's initial aiming direction recorded from the three dials*
$(\kappa_{XYZ}, \eta_{XYZ}, \varphi_{XYZ})$	*The initial orientation of the XYZ coordinates*
Θ	*Target plane yaw angle around Z axis*
τ	*Target plane pitch angle around X axis*
ρ	*Target plane roll angle around Y axis*
α_i	*Vertical off-axis angles of the reference point* P_i
Φ_i	*Horizontal off-axis angle of the reference point* P_i
$(\Phi_{i,a}, \alpha_{i,a})$	*The initial aiming angles of the reference point* P_i *recorded on the side and base dials*
α_S *or* $\alpha_{S'}$	*Adjusted magnification of the lens for the target plane when the camera is focused at S, or S' , respectively*
$\Upsilon_{S,S'}$	*Distortion function corresponding to a target plane at distance S' for a lens that is actually focused at distance S*
$(\Delta X, \Delta Y, \Delta Z)$	*Measurement errors of the XYZ coordinates of the target point P*
$(\Delta\bar{X}, \Delta\bar{Y}, \Delta\bar{Z})$	*Average offset of the XYZ coordinates of the target plane*
0 (0, 0, 0)	*Zero point of the XYZ coordinates*
(A, B, C)	*Normal of the target plane* $AX + BY + CZ = 1$
$c(x_c, z_c)$	*Coordinates of the center of HDR images on the image plane xz, often at c (0, 0)*
c_S *or* $c_{S'}$	*Distance from the focal point O to the image plane of the target P, when the camera is focused at distance S, or S' , respectively*

CF	*Calibration factor of luminance mapping at a local point*
CF_{global}	*Global calibration factor with an average value of all local CFs*
d_i	*Distance of the reference point P_i to the camera's focal point O*
f	*Focal length of the lens*
h_{sensor}	*Height of the imaging sensor of the camera*
$k_1, k_2, k_3...$	*Coefficients*
$k_{1,S}, k_{2,S}, k_{3,S}$	*Coefficients, when the camera is focused at distance S*
$k_{1,S1}, k_{2,S1}, k_{3,S1}$	*Coefficients, when the camera is focused at distance S1*
$k_{1,S2}, k_{2,S2}, k_{3,S2}$	*Coefficients, when the camera is focused at distance S2*
$k_{1,S'}, k_{2,S'}, k_{3,S'}$	*Coefficients, when the camera is focused at distance S'*
L_{HDR}	*Luminance extracted from a pixel on the HDR image*
L_{meter}	*Luminance measured in the field using a meter*
LLF	*Light loss factor*
m	*Pixel width of an HDR image, e.g., 5184 pixels (reduced to 843)*
η	*Pixel height of an HDR image, e.g., 3456 pixels (reduced to 658)*
$O(X_0, Y_0, Z_0)$	*Focal point of the camera in XYZ coordinates*
$P(X, Y, Z)$	*Target point P in XYZ coordinates*
$P(X', Y', Z')$	*Target point P on the target plane in local coordinates X'Y'Z'*
$P(X_{cali}, Y_{cali}, Z_{cali})$	*Calibrated XYZ coordinates of the target point P*
$P_a (X_a, Y_a, Z_a)$	*Aiming point of the camera in XYZ coordinates*
$p_d(x_d, z_d)$	*Distorted geometric coordinates on the image plane xz of the image of the target point P*
$P_d(X_d, Z_d)$	*Distorted geometric coordinates on the target plane XZ of the target point P*

$P_i(X_i, Y_i, Z_i)$	*Reference point P_i in XYZ coordinates on the target plane, i = 1, 2, 3,...*
$P_i(X'_i, Y'_i, Z'_i)$	*Reference point Pi in local coordinates X'Y'Z' on the target plane, i = 1, 2, 3...*
$p_{pix}(x_{pix}, z_{pix})$	*Pixel coordinates on the HDR image of the image of the target point P*
$p_u(x_u, z_u)$	*Undistorted geometric coordinates on the image plane xz of the image of the target point P*
$P_u(X_u, Z_u)$	*Undistorted geometric coordinates on the target plane XZ of the target point P*
r_d	*Distorted distance(radius) on the image plane xz of the image of the target point P to the center c(0, 0)*
$r_{d,S}$, $r_{d,S1}$ *or* $r_{d,S2}$	*Distorted distance (radius) on the image plane xz of the image of the target point P to the center c(0, 0), when the camera is focused at distance S, S1, or S2, respectively*
r_i, g_i, b_i	*The input RGB values of a pixel on HDR images*
r_o, g_o, b_o	*The output RGB values of a pixel on HDR images*
r_u	*Undistorted distance (radius) on the image plane xz of the image of the target point P to the center c(0, 0)*
$r_{u,S}$, $r_{u,S0}$, $r_{u,S1}$ *or* $r_{u,S2}$	*Undistorted distance (radius) on the image plane xz of the image of the target point P to the center c(0, 0), when the camera is focused at distance S, S0 , S1 or S2, respectively*
S, S1 or S2	*Focusing distances of the camera*
S'	*Perpendicular distance of a target plane to the focal point O*
$t_1, t_2, t_3,...$	*Coefficients*
$t_{1,S1}, t_{2,S1}, t_{3,S1}$	*Coefficients, when the camera is focused at distance S1*
$t_{1,S2}, t_{2,S2}, t_{3,S2}$	*Coefficients, when the camera is focused at distance S2*
UCS	*User coordinate system*

$V(v)$	*Vignetting curve*
v	*Off-axis angle*
v_{S1}	*Calculated off-axis angle, when camera is focused at distance S1*
v_{S2}	*Calculated off-axis angle, when camera is focused at distance S2*
WCS	*World coordinate system*
w_{sensor}	*The width of the imaging sensor of the camera*
XYZ	*3D right-handed Cartesian coordinates XYZ in the field*
X' Y' Z' or X' Z'	*Local coordinates of the target plane*
xz	*Image plane xz located on the imaging sensor of the camera*
$(x_{c,pix}, z_{c,pix})$	*Pixel coordinates of the image of the center of the HDR image*
$(x_{u,S'}, z_{u,S'})$	*Undistorted geometric coordinates of the image of the target point P on the image plane xz, when the camera is focused on S'*
y%	*Luminance mapping errors in percentage*

TABLE OF CONENTS

LIST OF FIGURES

LIST OF TABLES

CHAPTER 1: INTRODUCTION

1.1 Background

Daylight has a major effect on energy consumption with its ability to reduce the use of artificial lighting. Building designers and owners often strive to allow more daylight to penetrate the space on a given day with appropriate day lighting controls in place. The Commission Internationale del'Enclairage (CIE) published a standard addressing the modeling of the spatial distribution of daylight. This standard (CIE S011/E: 2003) [1] assumes that the luminance distribution of the sky is asymmetrical about the solar meridian, and the sky conditions cover 15 different models in terms of the cloud coverage. The 15 different types of sky conditions are represented in Table 1 on the following page. This table illustrates the various environments that make up the numerous sky modeling conditions. As seen in the descriptions for each type, the sky conditions are described in a very general form, which does not leave much room for the inevitable variations seen throughout a typical day. With the sky and the sun changing every second during real-time measurements, it is hard to justify the accuracy of these 15 types of skies. In other words, more detailed studies should be completed to address this issue and further advance the sky modeling criteria.

Table 1: 15 Types of CIE Sky

CIE Sky Type	Gradation	Description of Luminance Distribution
1	I	CIE standard overcast sky, alternative form with steep luminance gradiation toward zenith, azimuthal uniformity
2	I	Overcast, with steep luminance gradation and slight brightening toward the Sun
3	II	Overcast, moderately gradewd with zimuthal uniformity
4	II	overcast, moderately graded, snad slight brightening toward the Sun
5	III	Sky of uniform luminance
6	III	Partly cloudy sky, no gradation toward zenith, slight brightening toward the Sun
7	III	Partly cloudy sky, no gradation toward zenith, brighter circumsolar region
8	III	Partly cloudy sky, no graduation toward zenith, distinct solar corona
9	IV	Partly cloudy, with onscured Sun
10	IV	Partly cloudy, with brighter circumsolar region
11	IV	Wqhite-blue sky with distinct solar corona
12	V	CIE standard clear sky, low illuminance turbidity
13	V	CIE standard clear sky, low illuminance turbidity
14	VI	Cloudless turbid sky with broad solar corona
15	VI	White-blue turbid sky with broad solar corona

These 15 sky models are pre-defined and thus not "realistic" nor real-time climate-based. "Climate-based" daylight modeling has been a topic of research in the past decade [2]. The purpose is to provide more realistic sky conditions in terms of the daylight availability for a given location on a given day at a unique time. This type of information would be strictly based on either the real-time sky measurement or the historic data. Climate-based daylight modeling is constructed on location and meteorological data, which includes geographic coordinates, time of day, and variability of the weather conditions. It is important that the data that represent the modeled sky for daylighting be accurate to properly portray the conditions of the climate. Such accurate and reliable detail could play a major role in sustainable building design and future innovations. In addition, it is ideal for the data to be collected either in real-time or from historic data gathered over a long period of time to take into account the variability of the weather. This time period for historic data collection can be anywhere from a year to 30+ years for any climate-based modeling applications [3].

1.2 Current Technology

Currently, there are two methods for measuring the luminance of the celestial sky. The luminance of the sky can be measured using a conventional luminance meter or a sky scanner. The luminance meter is the more primitive method of the two with affordable cost, acceptable accuracy, but prone to human error. The meter measurement process is simply done by aiming a luminance meter such as the Minolta LS-100 (Figure 1) at the sky and manually measuring various target points throughout the sky. This is a very tedious and inefficient method with low measurement resolution. Also, the meter often

has limited measurement range that can only be used for measuring the sky luminance rather than the sun, which is too bright. In addition, this measurement technique yields results with a random layout of measurement points.

Figure 1: Minolta LS-100

The second existing method for measuring luminance of the sky can be done by using a sky scanner (Figure 2). This method incorporates the 145 Tregenza sky patches for collecting the data. Some of the downfalls that exist within this method include the limited amount of data collection available. The 145 Tregenza patches only cover approximately 2/3 of the total celestial hemisphere [4]. Therefore, there is a significant amount of data that go uncovered. In addition to the inability to retrieve data from all parts of the sky, the resolution of the sky scanner is relatively low and cannot measure the luminance of the sun.

Figure 2: MS-321LR Sky Scanner

Based on the two existing methods for measuring the luminance of the sky and sun and the shortcomings they are associated with, it is evident that a new technology was needed to obtain accurate data. High dynamic range (HDR) photography [5] and photogrammetry [6] were the likely choices to fill this gap. The camera-aided measurement technology combines a fast collection process in compliance with the real-time climate-based weather conditions and high measurement resolutions of the data points. However, the collected dataset is extremely large, which can have a negative effect on the data treatment stage of the research. Additionally, the camera-aided measurement of the sky and the sun has not been proven as accurate and reliable results [1]. The University of Kansas Lighting Research Laboratory is currently working on these issues to develop the camera-aid technologies for luminance mapping the sky and the sun.

Mapping the luminance distribution of the sky and the sun is critical for daylight harvesting. However, the two main technologies (sky scanner and luminance meter) commonly used today for these measurements are inefficient and lack the ability to accurately capture the varying nature of daylight. In addition, these equipments produce data with low measurement resolution and relatively long time lapse when obtaining the data during the field measurement. For instance, the resolution is 1 degree of the viewing angle of the photo sensor for the LS-100 luminance meter and 11 degrees for a typical sky scanner [6]. This resolution is relatively low for capturing the changing spatial distributions of the sky luminance, but could be improved to maximize the end results of the sky and the sun mapping process. In addition, measurement of the sun brightness is technically unfeasible with these two devices because of limited range of measurement. Neither the luminance meter nor the sky scanners are able to collect data directly from the sun that has a brightness of 1.6×10^9 cd/m^2 at noon. With certain methods, filters are switched in and out of the equipment to capture the sun [6]. This is time consuming throughout an experimental process and limits the sky mapping procedure, which has much lower luminance values compared to the sun. Furthermore, a typical sky scanner will only map 2/3 of the celestial hemisphere [5]. Within this method of data collection, valuable information is lost because the scanner is not able to render the entire upper hemisphere for the desired amount of information.

It could be ideal to maximize the measurement area of the celestial sky in which the data are obtained in high resolutions to truly represent the luminance distribution of the sky and sun over time and at different sites. Recent technological advances in high dynamic ranging imaging have brought us close to solving both of these issues [6]. In

particular, the KU Lighting Research Laboratory has come out with camera-array-based sky luminance mapping technology to capture the real-time luminance distributions of the sky and the sun [5]. The camera-array-aided method uses an XYZ coordinate system that essentially maps out the entire celestial hemisphere visible to the camera lens as it is extracted from the two cameras using HDR photogrammetry. Each data point is a pixel on the HDR image taken by the camera, containing both luminance and XYZ coordinates pertaining to the temp-spatial luminance distribution. In the field, the two Canon EOS cameras were set up to with one camera without a filter measuring the sky while the other camera was equipped with a neutral density filter of 1/1000 measuring the sun. Together, the low dynamic range photographs taken by both cameras were collected and generated into two HDR images through data fusion. Such HDR images were further treated using various tools and software such as Radiance®, Photosphere® and Luminance HDR to retrieve the luminance data. By replacing the luminance data of the sun and its corona on the HDR image taken with the sky-camera with those of the sun and its corona taken with the sun-camera, the luminance distribution of the entire celestial hemisphere was obtained. More information on the two trials that took place at Clinton State Park in Lawrence, KS can be found later in this paper. Once the HDR photography method is proven an accurate and efficient way to measure the luminance of the sky and the sun, the information collected through this method can be used for real-time climate-based modeling for daylight harvesting.

Based on previous studies with HDR photography, results have proven that this data-collection technique yields reliable results with adequate accuracy [7] for mapping

the luminance distribution of common objects and the sky but not yet proven for mapping highly bright light sources like the sun.

It is expected that with improvement like using neutral density filter of 1/1000, HDR photography may be used to measure the luminance of points across the entire celestial hemisphere, but research is being conducted in the KU Lighting Research Laboratory to validate it. The present study is a part of this research. This technology has also proven successful for uneven levels of light. This is crucial throughout the measurement of the sky with irregularities formed from cloud cover or asymmetric distribution of light.

One of the first studies dealing with HDR photography for luminance mapping the sky and the sun was completed by Stumpfel et al [8], who developed a method that used a combination of different aperture sizes and shutter speeds to measure the luminance of the sky and sun. The main equipment used in this process consisted of a single digital Canon EOS IDS fitted with a Sigma 8mm fisheye lens. In addition, a density filter was used behind the lens to temper the light entering the camera. This method using a single camera for collecting data was not as fast as the current camera-array based technology due to the switching of lenses and shutter speeds throughout the process. Needless to say, it still played a major role in the development of what camera-based sky mapping is today. Inanici [8] partook in a second research study that utilized HDR photography to measure the sky.

Figure 3 depicts the underlying HDR photogrammetry that was developed in the lighting research laboratory and is used in this study for acquisition of the XYZ coordinates of every single measurement data point on the celestial sky. Note that the

image portrays a generalized target on a target plane, but this technology can be used in any scenario including the target points on the celestial hemisphere. In this measurement method, one or more digital cameras are placed at the origin (0, 0, 0) and directed at the target. In the case of the luminance mapping of the sky, the camera(s) would be fitted with a circular fisheye lens. Figure 3 explains the positioning and direction of the camera(s) with the yaw (*k*), pitch (η), and roll (φ). Based on the previous research in the KU Lighting Research Laboratory [5], the average errors came out to be 1.8% to 6.2% for luminance measurement of typical nonluminous surfaces and 12.9 to 24.3 mm for geometric measurement [6].

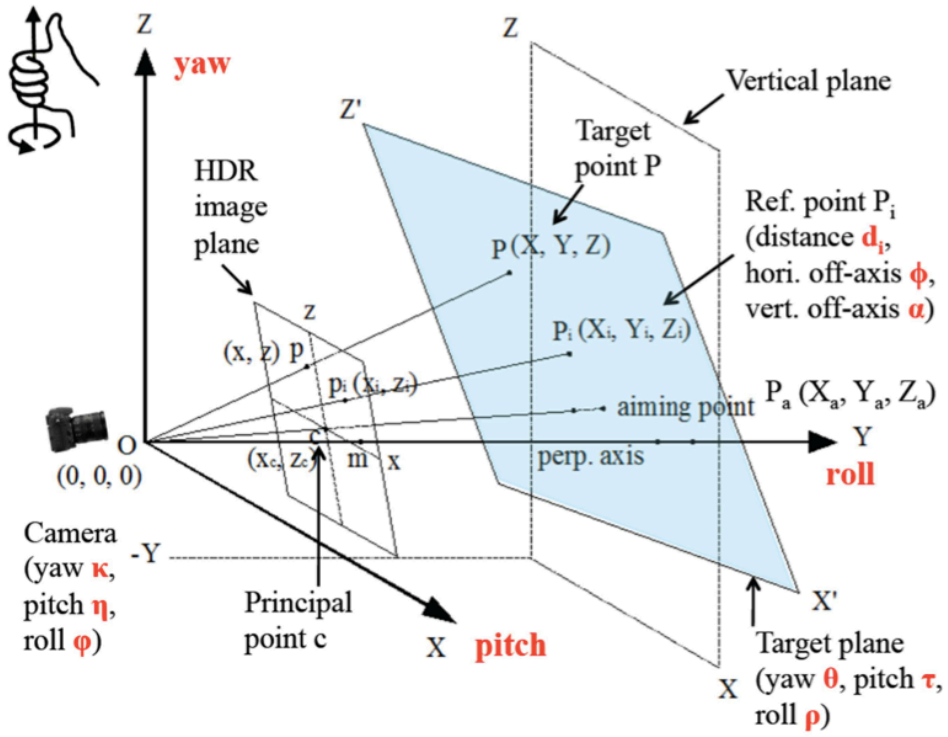

Figure 3: HDR Photogrammetry and Photogrammetric Coordinates [6]

These techniques were all used in the field measurement performed at Clinton State Park. The present study was aimed at exploring whether the pixel resolution could be reduced later in the laboratory from the original HDR images to condense the overwhelming workload of big data treatment. It was aimed to provide a more simplified set of collected data that could still accurately portray the luminance distribution of the sky and the sun in hopes of altering future studies with a more user-friendly approach. The reduction process was completed using the software Luminance HDR after the raw HDR images were generated in Radiance®. Another software, Photosphere®, was also used to validate that the reduction of pixels did not negatively affect the images from a visual standpoint.

In the field, two HDR images were generated using an array of two cameras, to measure the luminance of the sky and the sun, respectively. On each HDR image, a total of 18 million pixels were collected throughout the measurement process and calibrated to reveal the luminance distribution. With such large amounts of data, it was expected to yield very accurate results and as efficiently as possible. However, one main issue still remained with the collected big data. Given the limitations of current computing facilities, 18 million pixels on each HDR images and hundreds and thousands of HDR images obtained year around were far too difficult to manage when trying to complete this process in an efficient manner. To bring this technology to the forefront of luminance mapping, it was imperative to discover a simplified way to minimize the amount of data while still maintaining an adequate amount of information.

Daylight modeling is one aspect of design that is slightly slacking, and new technologies need to be implemented to keep up with the sustainability curve. The HDR photography and photogrammetry method is a new technology that has been studied in the past. This relatively new method has shown great promise in providing accurate data that can be geared towards climate-based modeling, yet still need validation in field studies. In addition, the HDR photography and photogrammetry method has posed three major concerns as follows:

1. Some studies have used a single, fixed aperture or multiple apertures of the same camera [5, 9]. Based on previous studies, it has been proven that using the single aperture minimizes the error of the lens for luminance acquisition. However, a recent study by Stumpfel et al [8] has shown that using a combination of multiple apertures through HDR imaging is possible at lowered accuracy, yet it can be time-consuming.

2. It is very difficult to capture both the sun and sky in an accurate and timely manner using a single camera. This is caused by the extreme brightness of the sun (1.6×10^9 cd/m^2). In past studies, filters were used on the camera equipment to help diffuse the light entering through the lens. Adjusting the cameras throughout the data collection process can impede the experiment.

3. HDR photography maps the luminance distribution of the sky and the sun. With high definition photographs, this means that millions of data points are

collected and attempted to be analyzed, resulting in big data. Too much data can have a negative impact on storage and data treatment given the limitation of current computing facilities.

1.3 Objectives and Research Scope

The present study was aimed at exploring the feasibility of reducing pixel resolution of raw HDR images for calibration of sky luminance measurements. This study could prove whether it is possible to reduce the workload in laboratory data treatment associated with the big data collected while maintaining reliable results. The current study was based on the existing technology of the lighting research laboratory [6] and attempted to simplify it for the end users in a resourceful manner as possible. The main issue that was addressed during this study was the reduction of the amount of big data collected throughout each experiment. When dealing with such large amounts of data, it is difficult to find the computational power to handle it by typical day lighting practitioners. Without reasonable storage capacity on average size computers, it is difficult to advance this technology into the hands of the users. To make this process user-friendly, it is important to find a way to make the collected data more manageable. It is necessary to reduce the big data for laboratory treatment while still maintaining accurate results before more powerful computing facilities are available to handle big data easily and reliably.

An experiment was carried out at the Clinton State Park in Lawrence, KS at 1:30 pm on October 4th, 2015 to evaluate the null hypothesis that reducing the pixel resolution

of the HDR images in the laboratory would not compromise the overall value of the obtained data. Two Canon digital cameras EOS Rebel T2i fitted with Sigma 4.5mm F2.8 EX DC HSM Circular Fisheye lenses were mounted side by side on a custom designed Sky Measurement Tripod Head to take measurements of the celestial sky using the HDR photography. One camera was mounted without a neutral density filter and was used to capture the luminance distribution of the sky while the other camera was equipped with a neutral density filter of 1/1000 and used to capture the luminance of the sun and its corona. Then, two HDR images were generated in the laboratory from the low dynamic range photographs taken by both cameras and synthesized to combine the entire dynamic range of the luminance of the sky and the sun. The luminance data embedded in each of the two HDR images were later extracted in Radiance® and outputted to Microsoft Access and Excel for the follow-up data treatment. In previous studies and also the present study, it was discovered that the amount of data obtained from the cameras was very large and nearly impossible to handle in Microsoft Access or Excel due to their limited computation capacity of 18 million rows of data.

This study then reduced such big data during the data extraction process in the laboratory by lowering the pixel resolutions of the raw HDR images obtained in the field. Using a software program known as Luminance HDR, the size of the HDR images was reduced from 18 million data points to merely 270,500 data points. This allowed for easier management of the collected data, and sped up the overall data treatment process given the limited computing capacity of most desktop or laptop computers. The reduced datasets were then treated using Excel spreadsheets containing pre-developed equations. Calibration Factor (CF) values were calculated by comparing the actual horizontal

illuminance measured using an illuminance meter to the calculated illuminance from the sky and sun luminance data embedded in the synthesized HDR image. The end result was the CF ratio derived from the test sky and sun conditions obtained during the experiment. This CF value was then applied to the treated data for photometrical calibrations to yield a more accurate result.

In theory, the CF ratio should be close to 1.0 indicating the robust data collection and treatment process was carried out with minimal error. If the CF ratio of illuminance values obtained in this experiment are too small or too large, the CF value may have a negative effect on the photometric data treatment, resulting in either too low or too high luminance values of the sky and the sun that are deviated from their true brightness. In the present study, the CF value obtained during the laboratory data treatment was close to 0.05, indicating the dataset was improperly manipulated during the reduction process of pixel resolutions. Photometric calibrations using such a CF value (0.05) would lead to extraction of only 5% of the true luminance distributions of the sky and the sun. As a result, it is deemed inappropriate to reduce the pixel resolution of raw HDR images in the laboratory after the field measurement, since such a reduction found in this study is associated with a loss of useful data for luminance mapping of the sky and the sun. Further research to be conducted in the Lighting Research Lab will evaluate two possible ways to solve this problem. The first solution is to capture the HDR images with lower pixel resolutions by directly adjusting the camera settings in the field, which is not the optimal solution but recommended given the otherwise resulting big data and the limitations of current computing facilities. The second method is to conduct the data

treatment in a more powerful computing software such as Matlab without reduction of the original 18 million pixels embedded in the HDR images.

CHAPTER 2: METHODOLOGY

2.1 Field Measurement

To test the feasibility of HDR image pixel reduction, two field measurements were performed at Clinton Lake State Park in Lawrence, KS (Figure 4). The two trials were completed on October 4th, 2015 starting at 1:30 pm. The sky conditions were relatively clear with blue skies with very little cloud cover. Clinton Lake State Park was chosen as the experiment location based on its flat surroundings and lack of obstructions. When mapping the sky with fisheye lenses, it was difficult to find an area with minimal trees or other structures that could block out vital parts of the sky. It was important to find an area that allowed for a complete and clear shot of the sky.

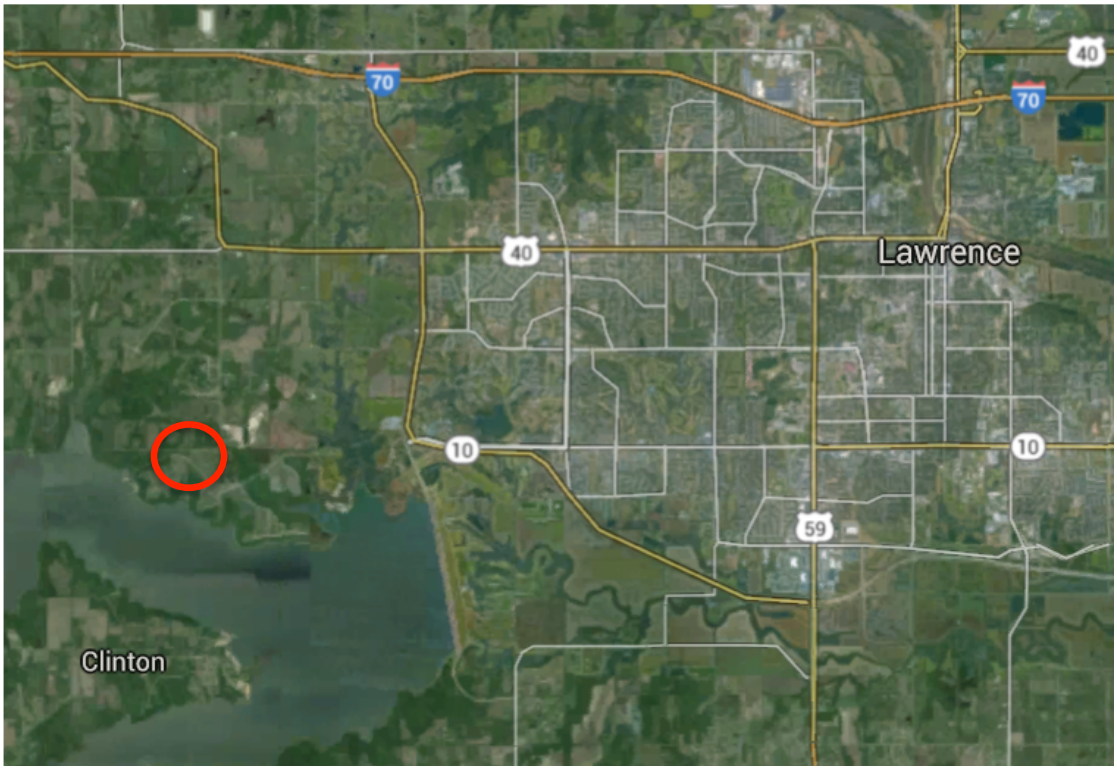

Figure 4: Aerial View of Clinton Lake State Park

Each trial utilized two Canon digital cameras, a tape recorder, a custom portable measurement platform – Sky Measurement Tripod Head – to mount the two cameras side by side, two laptop computers to control the cameras, a lux meter, Minolta T-10M, a lux meter sensor, an additional tripod to mount the video camera, a level, and a grey checker for calibration of the HDR photographing. Table 2 represents the equipment and settings used throughout Trial 1 and Trial 2 at Clinton Lake.

At the site, the equipment and meters were laid it out on the grass. The two Canon digital cameras EOS Rebel T2i fitted with Sigma 4.5mm F2.8 EX DC HSM Circular Fisheye lenses were mounted side by side on a custom designed Sky Measurement Tripod Head to take measurement of the celestial sky using the HDR photography. The level was used to make sure these two digital cameras were correctly mounted in the vertical position and aimed directly upwards. This maximized the field of vision of the two cameras and ensured adequate mapping of the sky and the sun. The second tripod was used to securely mount the video camera in place next to the tripod used for the two digital cameras. The video camera was an essential component used during the field experiment. Its main purpose was to film the entire data collection process as the cameras captured the images at the numerous exposures. The video was targeted at the lux meter to gather the real-time data. The Minolta T-10M was mounted directly to one of the tripod legs and equipped with a sensor. The sensor was routed up the leg of the tripod and mounted on the platform between the two digital cameras. It was important to mount this sensor in a location near the origin (between the cameras) at the XYZ coordinates 0, 0, 0 while avoiding any obstructions or shadows casted by the equipment. Lastly, the gray

checker was used for calibration purposes during the data treatment process. This practice has been consistent with all previous HDR studies.

Table 2: Equipment Summary [4]

Item	Value
Platform	Portable HDR photogrammetric Measurement Platform
Cameras	Two Canon cameras EOS Rebel T2i
Lenses	Two Sigma 4.5mm F2.8 EX DC HSM circular fisheye lenses
Neutral density filter	One Kodak No. 96 ND 3.00
Aperture size	f/22 (left, for measuring the sky), f/7.1 (right, for the sun)
Exposure time	1/15s to 1/2000s (left, sky), 15s to 1/4000s (right, sun)
Focus distance	0.24m
Lux meter	Minolta T-10M

This equipment worked together to map the overall luminance distribution of the sky and the sun. Once the low dynamic range photographs of the sky and the sun were collected by each camera, they were taken back to the laboratory for further data treatment. Using terminal language running on a Mac computer in the lighting research laboratory, those photographs were fused in Radiance® into two raw HDR images, including one HDR image for the sky (HDR_{sky}) and another HDR image for the sun (HDR_{sun}).

The purpose of the two separate trials was to compare the data against each other to make sure the equipment was functioning consistently and properly. Based on the clear sky conditions and the small amount of time that lapsed between each trial, the data should be relatively close. Even with the ever-changing luminance distribution from natural sunlight, the data should be accurate and reliable without any sharp differences between the two trials.

Figure 5 represents a schematic of the equipment set up. The left camera was mounted on the sky measurement tripod head and responsible for measuring the sky while the right camera equipped with a neutral density filter of 1/1000 was positioned to measure the sun. They were mounted in the vertical position to capture the entire sky dome with the circular fish eye lenses. Once the data was extracted, the sky plate was formed based on the (X, Y, Z) coordinate and their respective data points

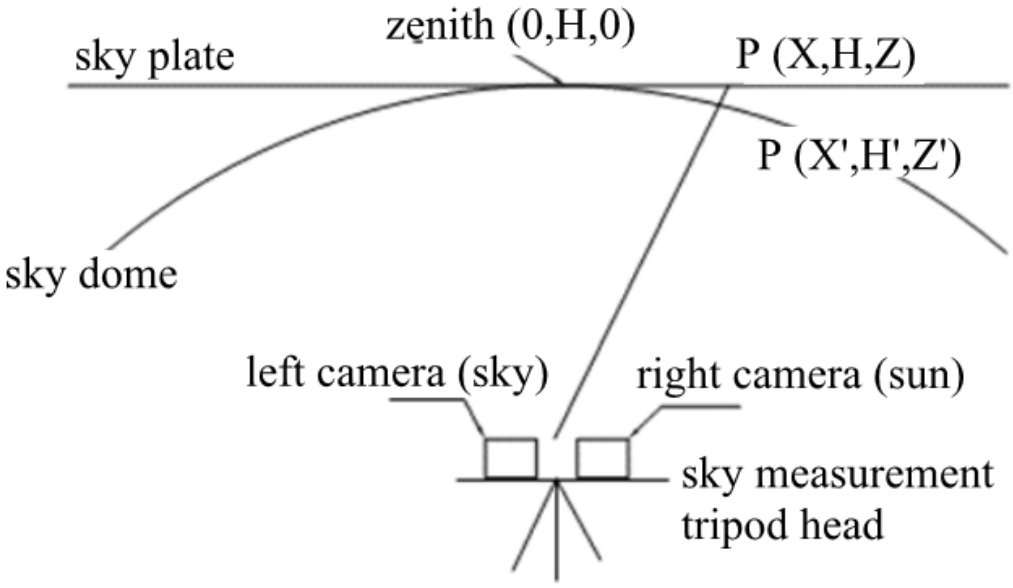

Figure 5: Luminance Distribution Mapping Diagram

Using two laptop computers connected to the cameras, the data process was started with two simultaneous keystrokes. As the two cameras captured images at various exposures, data were being collected from the sky and sun. This process was completed for each trial and the images were directly saved to the laptops' hard drives. Then, the two raw HDR images were generated later in the laboratory from both cameras and synthesized to combine the entire dynamic range of the luminance of the sky and the sun. The luminance data embedded in each of the two HDR images were extracted in Radiance® and outputted to Microsoft Access and Excel for the follow-up data treatment.

In addition to the data collected by the two digital cameras, the lux meter (Minolta T-10M, Figure 6) collected valuable real-time illuminance information. In the field, this device constantly measured the real-time horizontal illuminance with a small remote sensor mounted between the cameras. The readings were gathered as the two digital cameras simultaneously captured the images. Together these measurements would play a crucial roll towards the end of the data treatment process when determining the CF value. In total, 18 images were captured at various exposure times for each of the two trials. Further detail will be described in section 2.3.

Figure 6: Minolta T-10M

The camera-array-based measurement technique is very beneficial for mapping the luminance distribution of the sky and the sun [5]. With ever-changing lighting conditions from cloud cover and uneven sunlight, the dynamic range of the sky and the sun is very wide. As a benchmark, it can be said that the luminance of the sun is up to 1.6 x 10^9 cd/m^2. Likewise, it can be assumed that the sky can be measured between the range of 1 x 10^3 and 1 x 10^5 cd/m^2 depending on the conditions. Once the data are calibrated, the field measurement data are used to calibrate the calculation results by comparing to those values to determine if there were any errors that occurred throughout the experiment.

Figure 7 on the following page show the complete equipment setup used at Clinton State Park. It was important that all the equipment used throughout the present research study was consistent with previous studies completed by the lighting research laboratory. The general arrangement of each device used was photographed for future refrence and research studies.

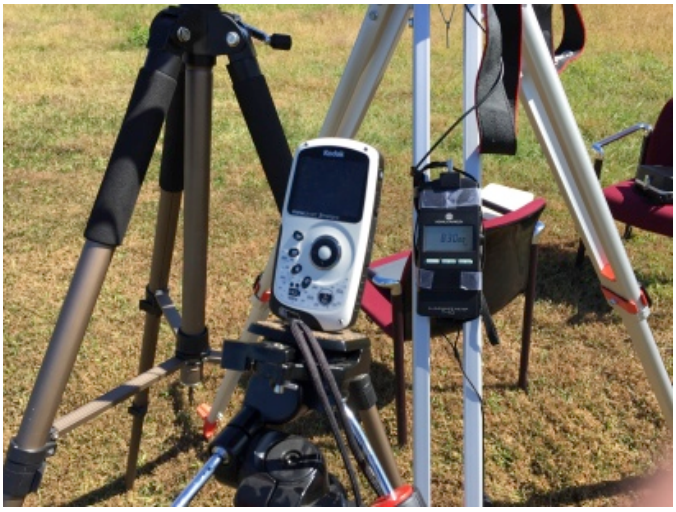

Figures 7: Equipment Setup

The cameras were setup beforehand for this experiment. The exposure time, aperture size, lenses and cameras were all pre-calibrated and determined based on previous research completed by the KU lighting research laboratory [5]. The Additive System of Photographic Exposure (APEX) [10] is dependent on the solar height, weather, cloud coverage, and other variables. Many factors come into play when determining the proper exposure for capturing the celestial hemisphere. Looking at Equation [1], the exposure value E_v can be determined [11]. This is based off the ratio of the aperture size and exposure time. This can be re-written using the scene luminance as seen in Equation [2], which relates the scene luminance (L_s) and the exposure value (E_v). These two equations were used in previous studies in the lighting research laboratory to determine the appropriate settings to be used on the two digital cameras.

$$2^{Ev} = \frac{N^2}{t} \qquad (1)$$

$$2^{Ev} = \frac{L_s S}{K_m} \qquad (2)$$

2.2 Laboratory Work

Once the data were extracted from the cameras and converted into an HDR image, the measurements were condensed by reducing the pixel count within the file. Each pixel represents a point filled with valuable information, so it was important to tabulate this newly reduced data in Microsoft Access and Microsoft Excel to be evaluated.

This process was completed by first extracting the raw images from the two Canon digital cameras. At various exposures, the low dynamic range photographs taken in the field were combined through data fusion to create two raw HDR images – HDR_{sky} and $HDR_{sun.}$ Together, these images represented the entire luminance distribution of the sky and sun with each pixel containing important data. Once the four (4) HDR images were obtained for the two trials completed at the Clinton Lake State Park, the images were uploaded to the Luminance HDR software. This software allows the user to scale the HDR images down by reducing the pixel resolution. By editing the images, the 18 million data points were reduced down to approximately 270,500. The next step was to take these new values and convert them into a text file that could later be imported into Microsoft Access and Excel. This conversion was done using Terminal Language on a MacBook computer. Microsoft Access was initially used to verify that the pixels were reduced to an appropriate amount. Access is much better at managing and storing the data, so using this software during the initial stages of the data evaluation was ideal.

Once the pixels were fully reduced down to 270,500 data points, they were copied into the Excel spreadsheet containing data treatment equations developed in previous studies [6, 12] and proven to be reliable and accurate. The end goal of the data treatment process was to calculate the Calibration Factor value. In previous research, the CF value has always been close to 1.0 which means very little calibration of the data was necessary. This emphasizes the fact that the data treatment in previous studies was done correctly and can be considered accurate. However, during this laboratory treatment of the present study, the CF value was closer to 0.05, which leads to a question whether it is

not feasible to reduce the pixel resolution of these raw HDR images while maintaining their accuracy of the luminance data of the sky and the sun.

2.3 Lab Data Treatment

Pre-developed equations (3) – (28) were used to treat the extracted luminance data. These equations and information were taken from previous studies [6] in the lighting research laboratory and proven to be successful. Among them, equations (3) – (15) were used in the present study for derivation of the XYZ coordinates in the real scenario from the xy pixel coordinates on the HDR image. Equations (16) – (28) in Appendix B were used to correct the lens distortion of the circular fisheye lenses used in the present study. This equations were developed in the KU Lighting Research Lab, and they have been proven successful on previous studies. The equations were incorporated into the excel spreadsheet in order to calibrate and test the reduced data set.

The data treatments were conducted in Excel spreadsheet for convenience of the present study. More sophisticated data treatments in MatLab will be worked out in the lighting research laboratory that is beyond the scope of this study. In this Excel spreadsheet, the xy coordinate of every single pixel on the HDR image was converted to the lens-distortion-corrected XYZ coordinates of the real scenario shown in Figure 7. Note that for convenience of the data synthesis later for capturing luminance distributions of the sky and the sun, we arbitrarily set the Z coordinate value on the sky plane as 8,000 m, which is the height of the top of the constant density atmosphere, covering the majority of clouds in the sky.

Meanwhile, in the Text file outputted from the HDR images, there is a column of brightness data B in addition to the xy coordinates of the pixels on the HDR images. An example of the text file is shown in Figure 8 in a portion. The brightness data of each pixel could be converted to its real luminance data on the sky when multiplied by a coefficient of 179, as shown in Equation (29).

B	Y	X
0.000e+00	256	355
2.523e+01	288	355
2.411e+01	320	355
1.426e+01	352	355
1.321e+01	384	355
1.199e+01	416	355
1.142e+01	448	355
1.146e+01	480	355
1.194e+01	512	355
1.269e+01	544	355
1.377e+01	576	355
1.497e+01	608	355
1.607e+01	640	355
1.821e+01	672	355
1.894e+01	704	355
2.051e+01	736	355
2.289e+01	768	355
3.028e+01	800	355
4.329e+01	832	355

Figure 8: A Portion of an Example Text File for Luminance Data

$$L = B * 179 \tag{29}$$

Such luminance data retrieved from the HDR images need photometric calibrations due to the possible measurement errors of the equipment and human errors in the field experiment. In this calibration, the measured iluminance (E_{meter}) of both the sky and the sun light was obtained as it arrived at the camera lens by using a lux meter. This value is then compared to the HDR luminance (E_{HDR}) that was calculated from the per-pixel luminance values of the entire celestial sky retrieved from the

HDR image using Equations (30) and (31) [13]. As a result, the Calibration Factor ($CF = E_{meter} / E_{HDR}$) was then used for calibrating the HDR images.

Equations to calculate the illuminance of the daylight from the sky:

$$dE = \frac{LRd\theta 2\pi R \cos\theta \cos(90 - \theta)}{R^2} \tag{30}$$

$$E = L2\pi \sin\theta \cos\theta * dseta \tag{31}$$

Where:

dE = illuminance from the point source in the sky with extension of dseta

L = luminance of the point source in the sky with extension of dseta

Seta = angle of elevation of the point source in the sky above the horizon

Delta-Seta = $180/(586^2)$ due to pixel loss during the reduction process

All data collected was worked into the spreadsheet to yield the CF values. The CF value was determined to be the deciding factor in whether this pixel reduction process was possible. In each HDR study, the CF value is intended to be close to 1.0. If the value strays too far above or below this value, it means that an error occurred and it is trying to over- or under-correct the yielded luminance value.

2.4 Feasibility Study

The main objective for this thesis study was to determine if altering the collected data in hopes to reduce the dataset would have a negative impact on the overall results. The pixel resolution of each image was reduced by grouping multiple pixels together and

essentially converting them to a single data point. This process is represented in Figure 9 on the following page.

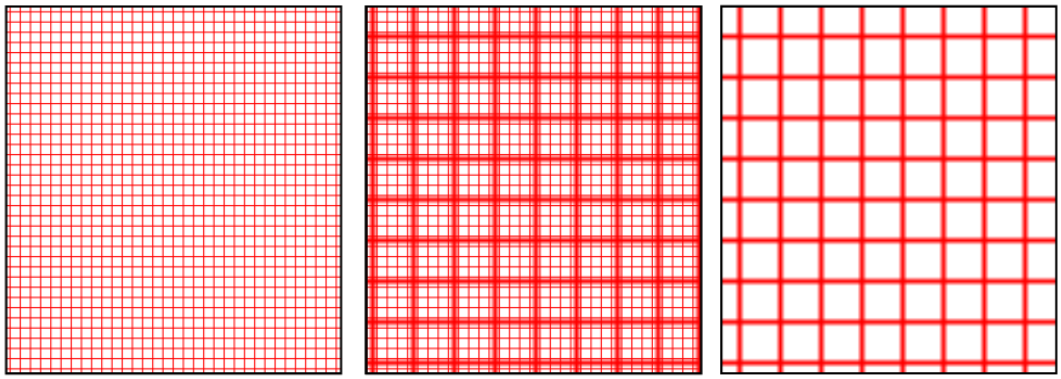

Figure 9: Pixel Reduction Process (Schematic)

As demonstrated in Figure 9, the congested grid on the left represents the initial data collection. As the pixels are reduced, they are grouped together and generalized while various data points are omitted. This process minimizes the amount of pixels within the image and can sometimes have a negative impact on the quality of the image. However, for the purpose of this study, the main objective was to determine if the data treatment process could be carried out with fewer data points. Using the HDR Luminance software, the four HDR images were converted to a lower pixel resolution. During this step in the experiment, the collected data points were reduced from 18+ million to approximately 270,500 points. This number was chosen to allow for adequate management of the data. The issue with leaving the data in its entirety is that it is hard for an average computer to process the information. This experiment used Microsoft Access and Microsoft Excel to treat the data. In past studies, it has proven to be difficult to calibrate the data when there are that many points. In order to advance this technology

further into the hands of other researchers and designers, it is necessary to make it functional with these programs. The only way to solve this problem is to find a way to reduce these files, which the current study attempted to accomplish.

Once the raw HDR images were reduced, the data was extracted from the four images into separate text files. These measurements were taken into Microsoft Access and populated into a table for review. Within these tables, the pixel coordinates and brightness were uploaded and plugged into the existing equations. The end result (X_m, X_m, X_m) was obtained and extracted into another excel spreadsheet. This spreadsheet, which will be referred to as the "Corrected Data", took the raw information obtained from the HDR image text file and corrected the values. The main purpose of this spreadsheet was to adjust the (X, Y, and Z) coordinates to account for the gap between to the two cameras. After this, the CF value, L_{HDR}, and $L_{calibrated}$ were calculated as seen in Table 3. L_{HDR} is the non-calibrated luminance of the celestial hemisphere at a given point. The CF value corrects the data based on the actual field measurement values obtained from the luminance meter that was mounted on the tripod (Figure 8).

Table 3: Calibrated Data (Partial)

		Input	derivation	derivation	derivation	derivation	Input	Input							
x	y	B	X m	Y m	Z m	$X_{corrected}$	$Y_{corrected}$	$Z_{corrected}$	Θ (rad)	delta-Seta n rad	E	Sum E	CF	L_{HDR}	$L_{Calibrated}$
658	537	6.994	-1544804.685	-953451.012	8759.259	-1544804.675	-953451.0125	8000.000	0.004	0.001	0.000102	1554499.74	0.051928603	1251.93	65.01076843
658	538	14	-383461.289	-236468.195	8188.306	-383461.280	-236468.195	8000.000	0.018	0.001	0.000819			2506.00	130.1330795
658	539	16.13	-219924.779	-135503.823	8107.905	-219924.769	-135503.8228	8000.000	0.031	0.001	0.001644			2887.27	149.931898
658	540	16.25	-154667.353	-95214.257	8075.822	-154667.344	-95214.25726	8000.000	0.044	0.001	0.002353			2908.75	151.0473244
658	541	16.28	-119562.263	-73539.923	8058.562	-119562.254	-73539.92319	8000.000	0.057	0.001	0.003046			2914.12	151.326181
658	542	16.32	-97631.185	-59998.872	8047.779	-97631.176	-59998.87225	8000.000	0.070	0.001	0.003734			2921.28	151.6979898
658	543	16.5	-82628.374	-50735.153	8040.402	-82628.364	-50735.15287	8000.000	0.082	0.001	0.004453			2953.50	153.3711294

CHAPTER 3: DATA ANALYSIS & RESULTS

As briefly mentioned in Chapter 2, many steps were taken in order to fully analyze the data and results of this research topic.

The first major step once the image resolution was reduced was to convert the data obtained into text files (.txt) that could be imported into Microsoft Access. Through this, the data was considered properly reduced and consolidated down to the point where it would be feasible to manipulate it in Microsoft Excel. Hence, the data was copied over to the Excel database that contained all previously developed equations. The data imported from the text files for each image contained the X-coordinate, Y-coordinate and brightness. For this experiment, the Z-coordinate was assumed to be 8,000 meters, which is the appropriate elevations for obtaining these data values. The first Excel database took the imported values and treated them through numerous equations. The Excel file used for this process can be referenced electronically with the equations taken from previous studies [6, 12].

The desired derivations at the end of the first spreadsheet were the corrected X, Y and Z coordinates in metric form (meters). Partial results for Trial 1 (Sky) can be seen in Table 4. As demonstrated in these results, the Z coordinate is relatively close to 8,000 meters but varies for each set of points. In the second stage of data treatment, this value is corrected and changed to 8,000 meters.

Table 4: Data Treatment (Partial)

X m	Y m	Z m
-1544804.685	-953451.012	8759.259
-383461.289	-236468.195	8188.306
-219924.779	-135503.823	8107.905
-154667.353	-95214.257	8075.822
-119562.263	-73539.923	8058.562
-97631.185	-59998.872	8047.779
-82628.374	-50735.153	8040.402
-71717.435	-43997.654	8035.037
-63424.351	-38876.357	8030.958
-56907.196	-34851.480	8027.753
-51650.124	-31604.555	8025.168
-47319.437	-28929.564	8023.037
-43689.708	-26687.337	8021.252
-40603.162	-24780.466	8019.733
-37946.069	-23138.737	8018.426
-35634.372	-21710.256	8017.288
-33604.603	-20455.841	8016.290
-31807.942	-19345.351	8015.405
-30206.219	-18355.221	8014.617
-28769.161	-17466.761	8013.909
-27472.445	-16664.956	8013.271
-26296.308	-15937.604	8012.692
-25224.524	-15274.688	8012.164
-24243.641	-14667.904	8011.680
-23342.420	-14110.313	8011.236
-22511.390	-13596.069	8010.827
28030.992	17516.011	7986.052

The second stage of the data treatment process can be referred to as the "Corrected Data". This data aimed to complete the data treatment process by using the corrected (X, Y, Z) coordinates along with the brightness, Θ, and luminace and comparing that to the field measurements obtained with the Minolta T-10M. Through this process, the Calibration Factor (CF) is derived as demonstrated in Table 5.

Table 5: Corrected Data Results (Partial)

B	X m	Y m	Z m	$X_{corrected}$	$Y_{corrected}$	$Z_{corrected}$	Θ (rad)	delta-Seta n rad	E	Sum E	CF	L_{HDR}	$L_{Calibrated}$
6.994	-1544804.685	-953451.012	8759.259	-1544804.675	-953451.0125	8000.000	0.004	0.001	0.000102	1554499.74	0.051928603	1251.93	65.01076843
14	-383461.289	-236468.195	8188.306	-383461.280	-236468.195	8000.000	0.018	0.001	0.000819			2506.00	130.1330795
16.13	-219924.779	-135503.823	8107.905	-219924.769	-135503.8228	8000.000	0.031	0.001	0.001644			2887.27	149.931898
16.25	-154667.353	-95214.257	8075.822	-154667.344	-95214.25726	8000.000	0.044	0.001	0.002353			2908.75	151.0473244
16.28	-119562.263	-73539.923	8058.562	-119562.254	-73539.92319	8000.000	0.057	0.001	0.003046			2914.12	151.326181
16.32	-97631.185	-59998.872	8047.779	-97631.176	-59998.87225	8000.000	0.070	0.001	0.003734			2921.28	151.6979898
16.5	-82628.374	-50735.153	8040.402	-82628.364	-50735.15287	8000.000	0.082	0.001	0.004453			2953.50	153.3711294
21.66	-71717.435	-43997.654	8035.037	-71717.426	-43997.65404	8000.000	0.095	0.001	0.006722			3877.14	201.3344644
33.01	-63424.351	-38876.357	8030.958	-63424.341	-38876.35683	8000.000	0.107	0.001	0.011558			5908.79	306.835211
33.34	-56907.196	-34851.480	8027.753	-56907.186	-34851.48033	8000.000	0.119	0.001	0.012977			5967.86	309.9026336
33.32	-51650.124	-31604.555	8025.168	-51650.114	-31604.55486	8000.000	0.131	0.001	0.01425			5964.28	309.7167292
33.96	-47319.437	-28929.564	8023.037	-47319.427	-28929.56443	8000.000	0.143	0.001	0.015804			6078.84	315.66567
33.79	-43689.708	-26687.337	8021.252	-43689.698	-26687.33662	8000.000	0.155	0.001	0.016976			6048.41	314.0854826
34.02	-40603.162	-24780.466	8019.733	-40603.153	-24780.46564	8000.000	0.167	0.001	0.018325			6089.58	316.2233832
33.67	-37946.069	-23138.737	8018.426	-37946.059	-23138.73678	8000.000	0.178	0.001	0.019334			6026.93	312.9700562
34.47	-35634.372	-21710.256	8017.288	-35634.362	-21710.2564	8000.000	0.189	0.001	0.020994			6170.13	320.4062322
34.74	-33604.603	-20455.841	8016.290	-33604.593	-20455.84135	8000.000	0.201	0.001	0.022343			6218.46	322.9159415
34.92	-31807.942	-19345.351	8015.405	-31807.932	-19345.35123	8000.000	0.212	0.001	0.023623			6250.68	324.5890811
25.36	-30206.219	-18355.221	8014.617	-30206.210	-18355.22126	8000.000	0.223	0.001	0.017983			4539.44	235.7267783
18.79	-28769.161	-17466.761	8013.909	-28769.151	-17466.76112	8000.000	0.233	0.001	0.013923			3363.41	174.6571831

The data obtained and represented in Table 5 show a CF value of 0.05. Due to the fact that this value is so low compared to 1.0, it can be said that this research was successful in proving that accurate results are unachievable when the pixel resolution of the HDR images are reduced. Proving this result further, the calibrated Luminance for the sky is shown in the column labeled $L_{calibrated}$. This value should be comparable to the values obtained over years of research. For example, the luminance of the sun is up to 1.6 x 10^9 cd/m^2. However, in this calibrated luminance data, the sun has a luminance of 18,749 cd/m^2, which is unlikely true under clear sky conditions in early afternoon (1:30 pm).There is a huge difference between the sun luminance obtained in this study with calibrations and 1.6 x 10^9. Likewise, it can be assumed that the sky can be measured between the range of 1 x 10^3 and 1 x 10^5 cd/m^2 depending on the conditions. These assumptions are far different from the results obtained in this experiment, thus further proving that this pixel reduction process is not possible and additional research needs to be completed.

The obtained CF value proved that it was not feasible to reduce the pixel resolution of the HDR image. This procedure had a negative effect on the calculations and created a CF value that was far too low. By yielding a CF value that was not close to 1.0, it was discovered that the L_{HDR} value was not formulated correctly. When calibrated with the CF value, the results are between 50 and 1,500 cd/m^2 for the sky and 2,000 and 20,000 cd/m^2 for the sun. When comparing these values with the actual readings of the sky and the sun (1 x 10^5 and 1 x 10^9, respectively) it is clear that they are not even close to being correct. Therefore it is safe to say that the feasibility study proved that you

cannot reduce the already created HDR image without having a negative impact on the end results.

CHAPTER 4: CONCLUSIONS & DISCUSSION

4.1 Conclusions

This research was conducted to find whether reducing pixel resolutions of HDR images in the post-processing laboratory stage is an efficient and reliable way to simplify the recent technological advances in luminance distribution sky mapping. The main objective behind this study was to help further develop this technology to a point where it was not only much more accurate than luminance meters and sky scanners on the market now, but also much more user-friendly and intuitive even with the accumulative big data collection and corresponding data treatment. Too much data can bog down an entire project, and it is important to simplify the post-processing data treatment of the original field measurements while still maintaining reliable results. This simplifies the overall process and allows the lighting society to easily apply these methods to a real project.

However, it was found that reducing pixel resolutions of the HDR images was not appropriate for data treatment while maintaining the accuracy, because of the data loss during the reduction stage. In this experiment, the pixels were reduced after the raw data was obtained and the raw HDR images (HDR_{sky} and HDR_{sun}) were created. This means that the data were collected before the photographs were reduced and that many data points were lost in the process. When trying to determine why this data loss occurred, it was discovered that reducing the resolution simply adjusted the pixel count instead of averaging (or blurring) the data together. Through the Luminance HDR software, each data point can be grouped into smaller grids that make up the entire 18 million pixel images. These groups can be simplified by extracting one pixel while omitting the rest. In other words, only one pixel from each group remains while the other data is thrown out.

For example, if a portion of a pixel grouping contains red, black, blue and yellow colored pixels, but this grouping of pixels is predominately black, then the image could be reduced to a single black pixel. This simplification process would take the red, blue and yellow pixels and throw them out while maintaining a single, black pixel. This holds true for the study at Clinton Lake State Park. Instead of averaging the data within each pixel grouping, one data point was selected to represent the entire portion. This issue caused for unreliable values and ultimately ended the study with data that could not be considered accurate.

There are various ways to obtain, treat and correct raw HDR data which means there are also various ways to manipulate it. Further research needs to be completed in order to narrow down the best method for reducing the pixel resolution without sacrificing the accuracy and reliability.

4.2 Discussion

Nonetheless, it is still possible that other methods could be useful in reducing pixel resolution of HDR images. Two proposed solutions were formed based on the results of the current study. The first solution is to capture the HDR images with lower pixel resolutions by directly adjusting the camera settings in the field, which is not the optimal solution but recommended given the otherwise resulting big data and the limitations of current computing facilities. The second method is to conduct the data treatment in a powerful computing software like Matlab without reduction of the original 18 million pixels embedded in the HDR images. Looking at the first proposed solution, it is recommended that the lighting research laboratory performs a study that reduces the

pixel resolution of the camera itself when the HDR images are taken. This method would ensure that the data points collected were already in the reduced format and there would not be any information lost in the post-field laboratory treatment. By reducing the pixels ahead of time, the calculations used throughout the data treatment phase would be functional and data points would not be thrown out, which compromises the pre-developed equations. However, this practical solution is not necessary or preferred when more powerful and faster computing facilities are available which can handle big data easier and faster.

It would be ideal to conduct a second experiment testing this method at a future date. The goal is to identify the highest pixel resolution of raw HDR images that current computing facilities could handle while still maintaining the highest measurement resolution. The camera will be set at a lower resolution to obtain a bit less data from the beginning. This would make treating the data much easier while still retaining all of the data points collected. It is important to note that the quality of the photograph would be lessened by the pixel reduction, but the equipment should still be able to accurately measure each point mapped throughout the sky. Another unsolved problem that remains is whether the effects of the reduction would be noticeable to the naked eye, or if the calibration factor would be compromised. These are all issues that could be addressed at a later date during the future study. In theory, this method should be successful as long as all of the data points obtained throughout the experiment are retained and could be efficiently treated by current computing facilities.

REFERENCES

[1] Commission Internationale del'Eclairage (CIE) S 011/E. 2003. Spatial distribution of daylight -CIE standard general sky.

[2] Mardaljevic, J.. 2006. Examples of climate-based daylight modelling. CIBSE National Con-ference 2006: Engineering the Future, 21-22 March, Oval Cricket Ground, London, UK.

[3] Gueymard C.A., Wilcox S.M. 2011. Assessment of spatial and temporal variability in the US solar resource from radiometric measurements and predictions from models using ground-based or satellite data. Solar energy 85, 1068-1084.

[4] Tregenza P.R. 1987. Subdivision of the sky hemisphere for luminance measurements. Lighting research and technology 19, 13-14.

[5] Cai H., Chung T.M. 2011. Improving the quality of high dynamic range images. Lighting Research and Technology, 43(1), 87-102.

[6] Cai. H. 2013. High dynamic range photogrammetry for synchronous luminance and geometry measurement." Lighting Research and Technology, 45(2): 230257.

[7] Stumpfel J, Jones A, Wenger A, Debevec P. 2004. Direct HDR capture of the sun and sky. 3rd International Conference on Virtual Reality, Computer Graphics, Visualization and Interaction in Africa. Cape Town, South Africa.

[8] Inanici, M. 2010. Evaluation of high dynamic range imaged-based sky models in lighting simulation. LEUKOS 7(2), 69-84.

[9] Inanici, M.N. 2006. Evaluation of high dynamic range photography as a luminance data acquisition system. Lighting Research and Technology 2006; 38: 123-136.

[10] Kerr, D. A.. 2007. APEX—The Additive System of Photographic Exposure, Issue 7.

[11] Hiscocks, P.D.. 2011. Measuring Luminance with a Digital Camera. Syscomp Electronic Design Limited. Sep.16, 2011. Extracted online from www.ee.ryerson.ca:8080/~phiscock/.../luminance-notes.pdf .

[12] Cai, H.. 2015. Solar design foundation: using high dynamic range photogrammetry for luminance mapping the sky and the sun. 2015 Architectural Engineering Institute Professional Conference, March 24-27, 2015, Milwaukee, WI.

[13] Hopkinson, Ralph Galbraith, P. Petherbridge, and James Longmore. Daylighting. London: Heinemann, 1966

Appendix A

Excel Data Treatment Results

Electronic files of the Excel Data are attached with this thesis and also available upon request

Appendix B

Pre-developed Equations

$$\begin{pmatrix} X_i \\ Y_i \\ Z_i \end{pmatrix} = \begin{pmatrix} d_i \cos\alpha_i \sin(-\phi_i) \\ d_i \cos\alpha_i \cos(-\phi_i) \\ d_i \sin\alpha_i \end{pmatrix} \tag{3}$$

$$\begin{pmatrix} A \\ B \\ C \end{pmatrix} = \begin{pmatrix} \dfrac{Y_1(Z_2 - Z_3) + Y_2(Z_3 - Z_1) + Y_3(Z_1 - Z_2)}{X_1(Y_2Z_3 - Y_3Z_2) + X_2(Y_3Z_1 - Y_1Z_3) + X_3(Y_1Z_2 - Y_2Z_1)} \\ \dfrac{Z_1(X_2 - X_3) + Z_2(X_3 - X_1) + Z_3(X_1 - X_2)}{X_1(Y_2Z_3 - Y_3Z_2) + X_2(Y_3Z_1 - Y_1Z_3) + X_3(Y_1Z_2 - Y_2Z_1)} \\ \dfrac{X_1(Y_2 - Y_3) + X_2(Y_3 - Y_1) + X_3(Y_1 - Y_2)}{X_1(Y_2Z_3 - Y_3Z_2) + X_2(Y_3Z_1 - Y_1Z_3) + X_3(Y_1Z_2 - Y_2Z_1)} \end{pmatrix} \tag{4}$$

$$\begin{pmatrix} \theta \\ \tau \\ \rho \end{pmatrix} = \begin{pmatrix} \arctan\left(-\dfrac{A}{B}\right) \\ \arctan\left(-\dfrac{C}{B}\right) \textit{ when } B \neq 0, \textit{ or } \arctan\left(\dfrac{C}{A}\right) \textit{ when } B = 0 \\ 0 \end{pmatrix} \tag{5}$$

$$S' = Y \cos\theta \cos\tau \tag{6}$$

$$\begin{pmatrix} x_d \\ z_d \end{pmatrix} = \begin{pmatrix} \left(x_{pix} - x_{c,pix}\right)\dfrac{w_{sensor}}{m} \\ \left(z_{c,pix} - z_{pix}\right)\dfrac{h_{sensor}}{n} \end{pmatrix} \tag{7}$$

$$\begin{pmatrix} X' \\ Y' \\ Z' \end{pmatrix} = \begin{pmatrix} r'_{11} & r'_{12} & r'_{13} \\ r'_{21} & r'_{22} & r'_{23} \\ r'_{31} & r'_{32} & r'_{33} \end{pmatrix}^{-1} \begin{pmatrix} X \\ Y \\ Z \end{pmatrix} \tag{8}$$

$$\begin{pmatrix} r'_{11} & r'_{12} & r'_{13} \\ r'_{21} & r'_{22} & r'_{23} \\ r'_{31} & r'_{32} & r'_{33} \end{pmatrix} = \begin{pmatrix} c\rho c\theta & -c\rho s\theta & s\rho \\ c\tau s\theta + s\tau s\rho c\theta & c\tau c\theta - s\tau s\rho s\theta & -s\tau c\rho \\ s\tau s\theta - c\tau s\rho c\theta & s\tau c\theta + c\tau s\rho s\theta & c\tau c\rho \end{pmatrix} \tag{9}$$

$$\begin{pmatrix} r'_{11} & r'_{12} & r'_{13} \\ r'_{21} & r'_{22} & r'_{23} \\ r'_{31} & r'_{32} & r'_{33} \end{pmatrix}^{-1} = \begin{pmatrix} r'_{11} & r'_{12} & r'_{13} \\ r'_{21} & r'_{22} & r'_{23} \\ r'_{31} & r'_{32} & r'_{33} \end{pmatrix}^{T} = \begin{pmatrix} c\rho c\theta & c\varpi s\theta + s\varpi s\rho c\theta & s\varpi s\theta - c\varpi s\rho c\theta \\ -c\rho s\theta & c\varpi c\theta - s\varpi s\rho s\theta & s\varpi c\theta + c\varpi s\rho s\theta \\ s\rho & -s\varpi c\rho & c\varpi c\rho \end{pmatrix} \tag{10}$$

$$\begin{pmatrix} X'_i \\ Y'_i \\ Z'_i \end{pmatrix} = \begin{pmatrix} r'_{11} & r'_{12} & r'_{13} \\ r'_{21} & r'_{22} & r'_{23} \\ r'_{31} & r'_{32} & r'_{33} \end{pmatrix}^{T} \begin{pmatrix} X_i \\ Y_i \\ Z_i \end{pmatrix} \tag{11}$$

$$\begin{pmatrix} X'_0 \\ Y'_0 \\ Z'_0 \end{pmatrix} = \begin{pmatrix} r'_{11} & r'_{12} & r'_{13} \\ r'_{21} & r'_{22} & r'_{23} \\ r'_{31} & r'_{32} & r'_{33} \end{pmatrix}^{T} \begin{pmatrix} X_0 \\ Y_0 \\ Z_0 \end{pmatrix} \tag{12}$$

$$\begin{cases} X' = X'_0 + (Y' - Y'_0)\dfrac{R_{11}x_u + R_{12}f + R_{13}z_u}{R_{21}x_u + R_{22}f + R_{23}z_u} \\ Z' = Z'_0 + (Y' - Y'_0)\dfrac{R_{31}x_u + R_{32}f + R_{33}z_u}{R_{21}x_u + R_{22}f + R_{23}z_u} \\ Y' = Y'_i \end{cases} \tag{13}$$

$$\begin{pmatrix} R_{11} & R_{12} & R_{13} \\ R_{21} & R_{22} & R_{23} \\ R_{31} & R_{32} & R_{33} \end{pmatrix}$$

$$= \begin{pmatrix} c(\varphi-\rho)c(\kappa-\theta) & -c(\varphi-\rho)s(\kappa-\theta) & s(\varphi-\rho) \\ c(\eta-\tau)s(\kappa-\theta)+ & c(\eta-\tau)c(\kappa-\theta)- & -s(\eta-\tau)c(\varphi-\rho) \\ s(\eta-\tau)s(\varphi-\rho)c(\kappa-\theta) & s(\eta-\tau)s(\varphi-\rho)s(\kappa-\theta) & \\ s(\eta-\tau)s(\kappa-\theta)- & s(\eta-\tau)c(\kappa-\theta)+ & c(\eta-\tau)c(\varphi-\rho) \\ c(\eta-\tau)s(\varphi-\rho)c(\kappa-\theta) & c(\eta-\tau)s(\varphi-\rho)s(\kappa-\theta) & \end{pmatrix} \tag{14}$$

$$\begin{pmatrix} X \\ Y \\ Z \end{pmatrix} = \begin{pmatrix} r'_{11} & r'_{12} & r'_{13} \\ r'_{21} & r'_{22} & r'_{23} \\ r'_{31} & r'_{32} & r'_{33} \end{pmatrix} \begin{pmatrix} X' \\ Y' \\ Z' \end{pmatrix} \tag{15}$$

$$r_d = k_1 \cdot v + k_2 \cdot v^3 + k_3 \cdot v^5 + k_4 \cdot v^7 + k_5 \cdot v^9 + \ldots \tag{16}$$

$$v = t_1 \cdot r_d + t_2 \cdot r_d^2 + t_3 \cdot r_d^3 + t_4 \cdot r_d^4 + t_5 \cdot r_d^5 + \ldots \tag{17}$$

$$r_u = f \cdot \tan(v) \tag{18}$$

$$r_{d,S1} = k_{1,S1} \cdot v + k_{2,S1} \cdot v^3 + k_{3,S1} \cdot v^5 + k_{4,S1} \cdot v^7 + k_{5,S1} \cdot v^9 + \ldots \tag{19}$$

$$r_{d,S2} = k_{1,S2} \cdot v + k_{2,S2} \cdot v^3 + k_{3,S2} \cdot v^5 + k_{4,S2} \cdot v^7 + k_{5,S2} \cdot v^9 + \ldots \tag{20}$$

$$v_{S1} = t_{1,S1} \cdot r_{d,S1} + t_{2,S1} \cdot r_{d,S1}^2 + t_{3,S1} \cdot r_{d,S1}^3 + t_{4,S1} \cdot r_{d,S1}^4 + t_{5,S1} \cdot r_{d,S1}^5 + \ldots \tag{21}$$

$$v_{S2} = t_{1,S2} \cdot r_{d,S2} + t_{2,S2} \cdot r_{d,S2}^2 + t_{3,S2} \cdot r_{d,S2}^3 + t_{4,S2} \cdot r_{d,S2}^4 + t_{5,S2} \cdot r_{d,S2}^5 + \ldots \quad (22)$$

$$r_{u,S1} = f \cdot \tan\left(v_{S1}\right) \quad (23)$$

$$r_{u,S2} = f \cdot \tan\left(v_{S2}\right) \quad (24)$$

$$r_{u,S} = \alpha_s \cdot r_{u,S1} + \left(1 - \alpha_s\right) \cdot r_{u,S2} \quad (25)$$

$$\frac{r_{u,S'}}{r_{u,S}} = \frac{c_{S'}}{c_S} = \gamma_{S,S'} \quad (26)$$

$$r_{u,S'} = \gamma_{S,S'} \cdot r_{u,S} = \frac{\left(S - f\right)S'}{\left(S' - f\right)S} \cdot r_{u,S} \quad (27)$$

$$\begin{cases} x_{u,S'} = \dfrac{x_{d,S} \cdot r_{u,S'}}{r_{d,S}} \\ z_{u,S'} = \dfrac{z_{d,S} \cdot r_{u,S'}}{r_{d,S}} \end{cases} \quad (28)$$